Coherent effects in a nonlinear birefringent resonance impurity-doped fiber

Sergei O. Elyutin*
Department of Physics, Moscow Engineering Physics Institute, Moscow 115409, Russia
(Received 15 December 2007; published 15 July 2008)

The polarization and spatiotemporal dynamics of coherent pulses propagating in a doped birefringent nonlinear fiber are modeled with the inclusion of the local Lorentz field. The numerical solutions describe the full set of equations for circularly polarized components of a coherent optical pulse coupled to the inhomogeneously ensemble of doped resonance atoms. The local field is shown to degrade the stability of the 4π-decay process. The development of a steady-state signal from the series of multiple photon echoes generated in active fiber is observed in simulations.

DOI: 10.1103/PhysRevA.78.013821 PACS number(s): 42.65.Tg, 42.50.Md, 42.81.Dp

I. INTRODUCTION

A fiber doped by resonance impurities is an attractive object for investigation for many reasons. An implantation of the impurities can alter the optical properties of the fiber in the desired direction. A fiber doped by Er^{3+} ions can serve as an active medium for the fiber amplifier, if an external pumping is able to invert the population of resonance levels. A self-induced transparency (SIT), discovered in [1] in the bulk sample was the most impressive manifestation of the coherent optical pulse interaction with resonance atoms. The theoretical aspects of SIT in the doped fiber were discussed in [2,3], particularly in [2] the inverse scattering transformation method was applied to the coupled system of vector nonlinear Schrödinger (NLS) and Bloch equations in the problem of propagation and collision of polarized solitary pulses in doped fiber. After the publication of Nakazawa *et al.* [4,5], where SIT was observed experimentally in the Er^{3+}-doped fiber, the interest to the coherent propagation of the short optical pulses switched to the field of ultrashort pulse (USP) amplification [5–9], the search of new propagation regimes [10,11], and the analysis of further generalization of the models of resonance and nonresonance subsystems [12–14]. As for instance, in [15], the dynamics of USP was theoretically studied in quadratically nonlinear resonance plasmonic metamaterial. On the other hand, the perceptible detuning from resonance reduces the problem to the NLS equations with generally nonuniform coefficients [16].

The brightest demonstration of the coherent time delayed interaction of USP with resonant fiber was reported in [17,18] in the form of photon echo effect. Later, accumulated photon echo was experimentally obtained in the active fiber amplifier [19].

Optical fibers reveal the birefringence owing to their very nature. Each of the components of the polarized radiation propagates in fiber with its individual phase (and group) velocity. Therefore, the relationship between the polarization states varies and the vector of the electrical field may rotate in the course of pulse propagation. When the intensity of radiation reaches a sufficiently high level the nonlinear corrections to the refractive index starts playing noticeable role [20]. Consequently, the velocities of the different polarization modes of the pulse alter [21]. For such intensities Kerr cross modulation becomes sufficiently strong to make the birefringence a nonlinear process when the beat period may even grow in an unlimited way [22,23]. Under the certain high level of the input pulse power the nonlinear effects [24–28] can conquer the linear birefringence.

The recent technological development of photonic bandgap (PBG) optical fibers [29], where light is guided inside a hollow core by the mechanism of Bragg reflection, permits us to reduce the Kerr nonlinearity of the host material by several orders of magnitude with respect to conventional index guiding silica core fibers. Filling the core of the PBG fiber with a resonant atomic or molecular gas makes it practical to observe coherent wave propagation effects [30], such as electromagnetically induced transparency, over relatively long lengths [31,32]. Indeed, the nonlinear index coefficient of PBG optical fibers is several orders of magnitude smaller than that for conventional silica fibers [33].

The implantation of resonance impurities alters the optical properties of fiber. If the duration of the pulse is much longer than polarization relaxation time and population difference relaxation time, then the additional absorption and saturation of absorption occur. The character of the absorption changes [34] if the pulse is shorter than the relaxation times. The absorption decreases with the increase of pulse amplitude until a complete vanishing, when the SIT conditions are achieved. If the energy levels of the doped atoms are degenerated over the projections of angular momentum, the propagation conditions for different polarization modes may also be different leading to the additional birefringence. In the femtosecond range of pulse duration the difference in the group velocities of the polarization modes becomes sufficient. The pulse experiences a split into two diverging separated signals (the walk-off effect).

With the increase of impurity density beyond the gaseous concentration, just like the transfer to the greater magnitudes of dipole moments of resonance particle the necessity in accounting the near dipole-dipole interaction [35] arises. Such an interaction leads to the local field effect featured by the dynamical shift of resonance frequency proportional to the population difference [36]. Even for a wide inhomogeneous absorption line, such a frequency sweep can cause the partial loss of coherency. A competition between the dephasing and interatomic dipole-dipole interaction, causing the appropriate

*soelyutin@email.mephi.ru

detuning from resonance, leads to the incoherent soliton formation [37].

In the present paper the coherent transient effects accompanying the propagation of USP of polarized light in an optical birefringent and resonance impurity-doped fiber will be numerically considered. The model is described by the self-consistent system of the nonlinear equations for polarization components of optical field and an ensemble of two-level atoms. The energy levels are degenerate over projections of angular momentum j_a and j_b ($j_a=1$ and $j_b=0$). Disregarding the linear birefringence and the walk-off effect, the model reveals an example of a completely integrable system [2,3,12], where one could ideally observe the coexistence of self-induced transparency (SIT) and optical solitons [38]. But in realistic doped fibers for the moderately intense pulse it can hardly happen as the disparity in the spatial scales and the pulse energy for the SIT solitary waves and optical solitons in a nonlinear fiber is very substantial: one 2π SIT pulse corresponds to the hundreds of NLS solitons in power. This issue was extensively discussed in a series of papers [39–41].

The general problem then apparently reduces to two characteristic cases: (a) the weak effect of the resonant absorption and refraction on the coupled solitonlike pulse propagation in nonlinear birefringent fiber, and (b) the effect of linear and nonlinear birefringence on the coherent propagation of polarized solitary waves in a short fiber, when at least the dispersion of group velocities can be treated as a weak effect. This latter case is the main concern of the current paper.

The objective of this paper is to demonstrate how the endemic fiber host material attributes, birefringence, material dispersion, and Kerr nonlinearity, affect the spatiotemporal dynamics of the optical coherent effects. As the examples of such effects, the self-induced transparency and photon echo developing in an extended resonance inhomogeneously broadened medium will be considered.

In what follows the model will be formulated in the form of field equations for an ultrashort optical pulse propagating in fiber coupled to the system of Bloch equations for the resonance medium (Sec. II) via resonance polarization. The model includes a local field effect as a distinguishing feature, which is necessary to be reckoned with if the ultrashort vector solitary optical pulse travels throughout a dense resonance medium, i.e., the medium with a relatively high dopant concentration or/and a large value of impurity dipole moment. The numerical estimates of the observed effects (Sec. III) precede the discussion on the modeling of polarized solitary pulse propagation in a nonlinear resonant fiber (Sec. IV) supplemented with the demonstration of the multiple photon echo effect in an extensive nonlinear birefringent dispersive medium possessing resonance impurities (Sec. V).

II. POLARIZED WAVES IN CUBIC MEDIUM WITH RESONANT IMPURITIES

The model consists of an inhomogeneously broadened ensemble of two-level degenerate atoms coupled to the electromagnetic field in the dipole and semiclassical approximation. Atoms with the energy transition in resonance with the carrier frequency are embedded in a dispersive, birefringent host fiber, whose cubic-nonlinear (Kerr) response is instantaneous [42]. It is assumed that the dielectric medium is isotropic, third harmonic generation can be neglected, and the second-order nonlinear susceptibility is identically zero.

A. Field equations

The polarization state of electromagnetic wave evolution in fiber is described by a superposition of two linearly polarized electric fields. The directions of these linear polarizations are parallel to the principal axes x and y of the birefringent fiber, which are termed slow and fast axes. Following the detailed procedure stated in [20,43], one can derive the normalized field equations for the polarized optical pulse propagating in fiber in the form

$$i\frac{\partial e_{1,2}}{\partial \zeta}+i\frac{1}{\ell_g}\frac{\partial e_{2,1}}{\partial \tau}+\frac{1}{\ell_d}\frac{\partial^2 e_{1,2}}{\partial \tau^2}+\frac{1}{\ell_c}e_{2,1}+\frac{1}{3\ell_k}(|e_{1,2}|^2+2|e_{2,1}|^2)e_{1,2}+\left(\frac{Lq}{A_0}\right)P_{1,2}=0. \quad (1)$$

In the system (1) the quantities $e_{1,2}(\zeta,\tau)$ are the normalized counterrotating polarization components of the field, $P_{1,2}(\zeta,\tau)$ is the resonance polarization of the impurities, ζ,τ-normalized spatial and temporal variables are connected with the physical values as $z=\zeta L$, $\tau=(t-z/v)t_0^{-1}$, t_0 is the characteristic time scale, which can be set either as the input pulse duration t_p or the time of the reversible relaxation of polarization T_2^*, and L is the normalizing length. The retarded time frame moves at the mean velocity v of the two polarization components of an optical pulse, i.e., $v^{-1}=(v_x^{-1}+v_y^{-1})/2$, and let $v_y>v_x$. Parameters $\ell_g,\ell_c,\ell_k,\ell_d$ are

$$\ell_g^{-1}=\frac{L}{L_g}=\frac{L}{2t_0}(v_x^{-1}-v_y^{-1}),\quad \ell_c^{-1}=\frac{L}{L_c}=\Delta\beta L,$$

$$\ell_k^{-1}=\frac{L}{L_k}=L\chi_{\text{eff}}\mu A_0^2,\quad \ell_d^{-1}=\frac{L}{L_d}=\frac{L}{t_{p0}^2}\frac{t_p^2}{t_0^2}|\sigma|. \quad (2)$$

The effective nonlinear interaction parameter χ_{eff} in Eq. (2) is the appropriate material susceptibility element averaged over fiber mode function.

In definitions (2) β_x (β_y) is the linear propagation constant of the slow (fast) mode of the birefringent fiber. We assume that the propagation constants slightly vary from some average value β such that $\beta_x=\beta+\Delta\beta$ and $\beta_y=\beta-\Delta\beta$. It is assumed for simplicity that the dispersion on both principal axes of the birefringent fiber is equal to $\sigma_x\approx\sigma_y=\sigma$, as well as coefficients $\mu_x\approx\mu_y=\mu$, where

$$\sigma_{x,y}=(1/2)d^2\beta_{x,y}/d\omega^2=\sigma,\quad \mu_{x,y}=\omega_0^2/2c^2\beta_{x,y},$$

and ω_0 is the carrier frequency.

Parameter q in the last term in Eq. (1) is responsible for the interaction of field with resonance atoms; $\boldsymbol{E}_0$ is the value of the normalizing field. The characteristic length of the fiber effects are

$$L_g = \frac{2v_1v_2t_0}{v_2 - v_1}, \quad L_c = \frac{1}{\Delta\beta}, \quad L_k = (\mu\chi_{\text{eff}}\boldsymbol{E}_0^2)^{-1}, \quad L_d = \frac{t_p^2}{|\sigma|}\frac{t_0^2}{t_p^2}, \tag{3}$$

The spatial length L_d parametrizes the dispersion of the group velocities. The polarization modes coupling is scaled by L_c. The corresponding terms in Eq. (1) couple the right and left circular components of the electromagnetic wave implying the linear birefringence effect. The nonlinear effects of self- and cross-modulation are revealed on the spatial length L_k. The difference of the group velocities causes a spatial divergence of the differently polarized components of the optical pulse (walk-off effect) on the characteristic length L_g.

B. Matter equations

Equations that describe the dynamics of the density matrix of the two-level atom, complement the system (1) to a full set of model equations. It is supposed that the energy levels of these atoms are degenerate over the projections of angular momentum, j_a and j_b, where subscripts a and b denote the upper and the lower energy states, respectively. For definiteness it is set that $j_a=1$ and $j_b=0$. For the slowly varying elements of density matrix $\hat{\rho}$, describing the transition between the two states $|a,m\rangle=|j_a=1,\ m=\pm 1\rangle$ and $|b\rangle=|j_b=0,\ m=0\rangle$, the following notations are introduced:

$$\rho_{12} = \langle a,-1|\hat{\rho}|a,+1\rangle, \quad \rho_{13} = \langle a,-1|\hat{\rho}|b\rangle,$$

$$\rho_{23} = \langle a,+1|\hat{\rho}|b\rangle,$$

$$\rho_{11} = \langle a,-1|\hat{\rho}|a,-1\rangle, \quad \rho_{22} = \langle a,+1|\hat{\rho}|a,+1\rangle,$$

$$\rho_{33} = \langle b|\hat{\rho}|b\rangle, \quad \rho_{kl} = \rho_{lk}^*, \quad l,k = 1,2,3.$$

Initial conditions are $\rho_{33}(0)=1$, $\rho_{22}(0)=\rho_{11}(0)=0$, $\rho_{12}(0)=\rho_{13}(0)=\rho_{23}(0)=0$. In terms of this quantum state basis, the resonant atomic transition $j_a=1\rightarrow j_b=0$ is characterized by the dipole momentum operator elements $d_{13}=d_{23}=d_{31}^*=d_{32}^*=d$.

In the dense resonant media [36] with a perceptible near-dipole-dipole interatomic interaction the Bloch equations for density matrix components should be modified to include the local field effect considering the difference between the macroscopic averaged field $e_\alpha(\zeta,\tau)$, which is coupled to the macroscopic polarization in the medium by Maxwell wave equations, and the microscopic local field $\tilde{e}_\alpha(\zeta,\tau)$, which drives the resonance atoms. The relationship between both fields is chosen in a simple Lorentz-Lorenz approximation [the last equation in Eqs. (4)], where structure factor η is determined by the properties of the resonance particle environment. It often contains a factor $4\pi/3$ attributed to the homogeneous distribution of dipoles in bulk samples. With the assumption that the pulse duration is much shorter than all irreversible relaxation times, the generalized system of Bloch equations can be written as follows:

$$\frac{\partial p_\alpha}{\partial\tau} = i\nu p_\alpha - if\Big(\sum_{\alpha'}\tilde{e}_{\alpha'}m_{\alpha'\alpha} - \tilde{e}_\alpha n\Big),$$

$$\frac{\partial m_{\alpha\alpha'}}{\partial\tau} = -if(\tilde{e}_\alpha^* p_{\alpha'} - \tilde{e}_{\alpha'}p_\alpha^*),$$

$$\frac{\partial n}{\partial\tau} = -if\sum_\alpha(\tilde{e}_\alpha p_\alpha^* - \tilde{e}_\alpha^* p_\alpha),$$

$$\begin{aligned}\tilde{e}_\alpha &= e_\alpha + (4\pi/3)n_a\boldsymbol{E}_0^{-1}\langle p_\alpha\rangle \\ &= e_\alpha + \boldsymbol{E}_{Lor}/\boldsymbol{E}_0\langle p_\alpha\rangle \\ &= e_\alpha + \eta\langle p_\alpha\rangle, \quad \alpha,\alpha' = 1,2.\end{aligned} \tag{4}$$

Here n_a is the concentration of the impurity atoms; the angle brackets $\langle\ \rangle$ mean the summation over all atoms with the frequency detuning $\nu=\Delta\omega t_0$ from the center of an inhomogeneously broadened line.

The new notations are introduced in Eqs. (4) as follows:

$$\rho_{12} = m_{21}, \quad \rho_{21} = m_{12}, \quad \rho_{11} = m_{11}, \quad \rho_{22} = m_{22},$$

$$\rho_{33} = n, \quad p_1 = -\rho_{13}, \quad p_2 = -\rho_{23},$$

with the initial conditions for the population of the ground level $n(0)=1$; for polarization, $p_\alpha(0)=0$, and it is set as $m_{\alpha\alpha'}(0)=0$. The Lorentz field correction, as is seen from Eqs. (4), causes the dynamical frequency shift proportional to the inversion in addition to the subsidiary nonlinearities introduced in coherent polarization. That can obviously lead to the partial loss of coherency in the pulse propagation and is able to affect the temporal form of the propagating pulses.

The dimensionless variables p_α in Eqs. (4) correspond to the polarization terms in Eq. (1) by the relationship

$$\left(\frac{Lq}{\boldsymbol{E}_0}\right)P_\alpha = \frac{L}{L_r}P_\alpha = \frac{L}{L_r}\langle p_\alpha\rangle = \frac{1}{\ell_r}\langle p_\alpha\rangle, \tag{5}$$

where $q=2\pi\omega_0 n_a d_{\text{eff}}/cn_{\text{ref}}(\omega_0)$, $L_r=fL_r^{(2\pi)}$. The characteristic length for an SIT 2π pulse to develop is

$$L_r^{(2\pi)} = (cn_{\text{ref}}\hbar)(\pi d_{\text{eff}}^2\omega_0 n_a t_0)^{-1}, \tag{6}$$

and the coefficient $f=d_{\text{eff}}\boldsymbol{E}_0 t_0 2^{-1}\hbar^{-1}=\boldsymbol{E}_0\boldsymbol{E}_{2\pi}^{-1}$ in the system (4) is an effective normalized frequency of oscillation of the material variables of resonance medium affected by the field of amplitude $\boldsymbol{E}_0$. Parameter $\boldsymbol{E}_{2\pi}$ is an amplitude of the SIT 2π pulse, d_{eff} means the dipole matrix element averaged over the fiber mode function, and n_{ref} is the refraction index of the host material.

The coupled system of Maxwell-Bloch equations (1) and (4) provides the mathematical basis for numerical simulation of the circularly polarized short pulses propagation in a nonlinear waveguide doped by resonance impurities. The systems (1)–(4) contain a certain complexity as the field $\tilde{e}_\alpha(\zeta,\tau)$, acting on an individual atom, depends in its turn on the averaged polarizability $\langle p_\alpha\rangle$, which makes the problem self-consistent. An application of the appropriate iteration procedure with the desired accuracy at the output permitted one to overcome this problem.

The results of calculations were the absolute value of the complex amplitudes $e_{1,2}(\zeta,\tau)$ of the counter-rotating right- and left-handed oppositely polarized fields. Following [21], the polarization state of the field in optical pulse was exam-

ined in terms of ellipticity $\varepsilon(\zeta,\tau)=(|\xi|-1)(|\xi|+1)^{-1}$ and azimuth angle $\varphi(\zeta,\tau)=\arg(\xi)/2$ between the axis of the polarization ellipse and the slow principal axis of the birefringent fiber, where $\xi=e_1e_2^{-1}$ is a complex quantity. The characteristic values of ε are $\varepsilon=0$ for the linear polarized light, $\varepsilon=+1$ for the purely right-hand circularly polarized light, and $\varepsilon=-1$ for the purely left-hand circularly polarized light. The launched pulses are assumed to have the *sech* form as follows:

$$e_{1,2}(0,\tau)=e_{m1,2}\ \mathrm{sech}[(\tau-\tau_0)/\delta],$$

where the dimensionless pulse duration $\delta=t_pt_0^{-1}$; τ_0 is the temporal coordinate of the center of the input pulse.

III. NUMERICAL ESTIMATES

The silica-based monomode fiber host material group velocity dispersion $D=4\pi c\sigma\lambda_0^{-2}$ [44] at $\lambda_0=1.55$ μm is typically $D=15$ ps nm^{-1} km^{-1}, the nonlinear index $n_2\approx10^{-13}$ CGS, then $\sigma=|d^2\beta/d\omega^2|/2\approx10^{-28}$ s^2 cm^{-1}. The nonlinear interaction parameter $\chi_{\mathrm{eff}}\approx n_2n_{\mathrm{ref}}/2\pi\approx2.3\times10^{-14}$ CGS. Then, with the input pulse duration $t_p=0.1$ ps, the dispersion length (3) is $L_d=t_p^2\sigma^{-1}\approx10^2$ cm. The polarization modes coupling effect reveals at the distance $L_c=(\Delta\beta)^{-1}\approx\lambda_0(2\pi\Delta n)^{-1}\approx25$ cm, where it is set as $\Delta n\sim10^{-6}$ [45].

The effect of group velocity mismatch becomes noticeable at the characteristic distance (3) $L_g=2v_xv_y(v_y-v_x)^{-1}t_p\approx2ct_p\Delta n^{-1}\approx6\times10^4$ cm. The spatial scale of the Kerr self- and cross-modulation process L_k (3) depends on the field amplitude $\boldsymbol{E}_0$: $L_k\approx n_{\mathrm{ref}}\lambda_0(\pi\chi_{\mathrm{eff}}\boldsymbol{E}_0^2)^{-1}$.

The balance between the fiber group-velocity dispersion and nonlinear pulse compression is achieved when $L_k=L_d$. That gives the value of the amplitude of the one-soliton solution of the NLS equation $\boldsymbol{E}_{\mathrm{NLS}}=(\sigma n_{\mathrm{ref}}\lambda_0)^{1/2}(\pi t_0^2\chi_{\mathrm{eff}})^{-1/2}\approx0.5\times10^4$ CGS for a 0.1 ps pulse duration. The corresponded length scale is $L_k^{(\mathrm{NLS})}\approx70$ cm. The NLS one-soliton peak intensity can be estimated as $I_{\mathrm{NLS}}=c(\boldsymbol{E}_{\mathrm{NLS}})^2/8\pi\approx4\times10^9$ W/cm^2.

We adopt the value of $d_{\mathrm{eff}}\approx5\times10^{-21}$ CGS (transition $^4I_{13/2}\rightarrow{}^4I_{15/2}$ in Er^{3+} ions) and the impurity concentration $n_a\approx10^{18}$ cm^{-3} that are valid for realistic samples [4]. Let us also set the value of the reversible relaxation time $T_2^*\approx t_0\sim0.1$ ps [6] encountered for the silica glass environment.

The quantity $L_r^{(2\pi)}=(n_{\mathrm{ref}}\hbar\lambda_0)(2\pi^2n_ad_{\mathrm{eff}}^2t_0)^{-1}\approx5\times10^2$ cm is the distance in the resonance sample, where the reciprocal reaction of the medium in the form of polarization and population differences develops to produce a number of coherent transients such as self-induced transparency (SIT) [1], photon echo [17–19], optical nutations, and breather waves. For the signals with a small pulse area [34,46] θ parameter $L_r^{(2\pi)}$ serves as the length of absorption. The pulse area of the NLS soliton is extremely small $\theta_{\mathrm{NLS}}=\pi d_{\mathrm{eff}}\hbar^{-1}t_0\boldsymbol{E}_{\mathrm{NLS}}=3\times10^{-3}\pi$ in comparison with $\theta_{\mathrm{SIT}}=2\pi$. The amplitude of a 0.1 ps 2π pulse is $\boldsymbol{E}_{2\pi}=2\hbar d_{\mathrm{eff}}^{-1}t_0^{-1}\approx4\times10^6$ CGS. The peak intensity of the pulse reaches the magnitude of $I_{2\pi}\approx2\times10^{15}$ W/cm^2. This well-known result [4] implies that the SIT soliton requires a power approximately six orders of magnitude larger than that for the NLS soliton, or that one 2π SIT pulse corresponds to the hundreds of NLS solitons by power.

As soon as the resonance interaction is considered as the basic effect, it is convenient to set the resonance absorption length as a characteristic spatial scale $L_r=fL_r^{(2\pi)}=L$, with the appropriate choice of normalizing field $\boldsymbol{E}_0=\boldsymbol{E}_{2\pi}(f=1)$. If, in spite of the evident discrepancy in pulse power, we assume that the fundamental NLS soliton is concurrently the SIT 2π pulse, then the condition $d_{\mathrm{eff}}\boldsymbol{E}_{\mathrm{NLS}}t_0\hbar^{-1}>2$ holds. The latter imposes a stringent restraint on the relationship between material constants $d_{\mathrm{eff}}\hbar^{-1}(\lambda_0\sigma\pi^{-1}\chi_{\mathrm{eff}}^{-1})^{1/2}>2$, followed by an exotic length of resonance absorption for the chosen concentration of the active centers $L_r^{(2\pi)}=n_{\mathrm{ref}}\lambda_0^2\sigma(8\pi^3n_at_0\chi_{\mathrm{eff}}\hbar)^{-1}\approx8\times10^{-3}$ cm. For the above characteristic values of the material constants the effective dipole moment $d_{\mathrm{eff}}=2\hbar(\pi\chi/\sigma n\lambda_0)^{1/2}\approx3.5\times10^{-18}$ CGS exceeds the referred value [4] by more than three orders. Only by assuming the concentration of the resonance impurities to be $n_a\sim10^{14}$ cm^{-3}, can one obtain a more or less reasonable value of $L_r^{(2\pi)}\sim80$ cm. An additional condition of the balance between Kerr nonlinearity and the dispersion broadening ($L_k=L_d$) leads to the final estimate $L_k=L_d\sim100$ cm, $L_c\sim24$ cm, and $L_g\sim6000$ cm. The relative parameters then are $\ell_d=\ell_k\sim1.25$, $\ell_c\sim0.3$, $\ell_r\sim1.0$, $\ell_g\sim75$, $f=1.0$, and $\boldsymbol{E}_0=5\times10^4$ CGS. The numerical modeling of such a complete situation will be presented later in Sec. V (Fig. 11).

The coherent effects in doped fibers, such as self-induced transparency, 4π-pulse breakup, π-pulse amplification [4,5], and photon-echo effect [18,19] were observed experimentally in the meter range fiber length. In [4,5] Nakazawa with co-workers used the excitation pulses with several hundred ps duration to reduce the high intensity of the SIT 2π pulses. Moreover, in order to observe pure SIT and to remove multiple NLS soliton effect, the fiber with low dispersion was chosen in experiments. However, in line with the scope of the current paper, the subpicosecond pulse duration domain is more interesting as the dispersion may not always be considered as the negligible effect then and, besides that, the excitation pulses duration is getting comparable with the inhomogeneous lifetime T_2^*. The above-mentioned problems in numerical estimates, which evidently arise in this range of pulse parameters, could be eased off by an appropriate selection of fiber host material and by the sort of dopant, e.g., by reducing the nonlinear interaction parameter χ and/or by manipulating the dispersion parameter σ.

The normalized Lorentz field correction η [Eq. (4)] can be estimated in terms of "co-operative" time $t_{cp}=\hbar(4\pi n_ad_{\mathrm{eff}}^2)^{-1}$, which is the time the polarization induced by the field of the traveling pulse in an ensemble of two-level systems emerges, and the characteristic time of the problem t_0, namely, $\eta=\boldsymbol{E}_{\mathrm{Lor}}/\boldsymbol{E}_{2\pi}=(4\pi/3)(t_0/8\pi t_{cp})$. The value of this parameter is not very large in a subpicosecond domain unless there is a very large magnitude of dipole moments inherent to such objects as quantum dots. In the following numerical analysis, in order to make effects more perceptible, the Lorentz correction reaches the value of several units. The previously cited numerical estimates imply that the conditions for observation of the distinctive nonlinear propagation effects do not generally match to parameters under which the pronounced coherent transients evolve. The numerical simulations, which follow in the next section, are focused on the

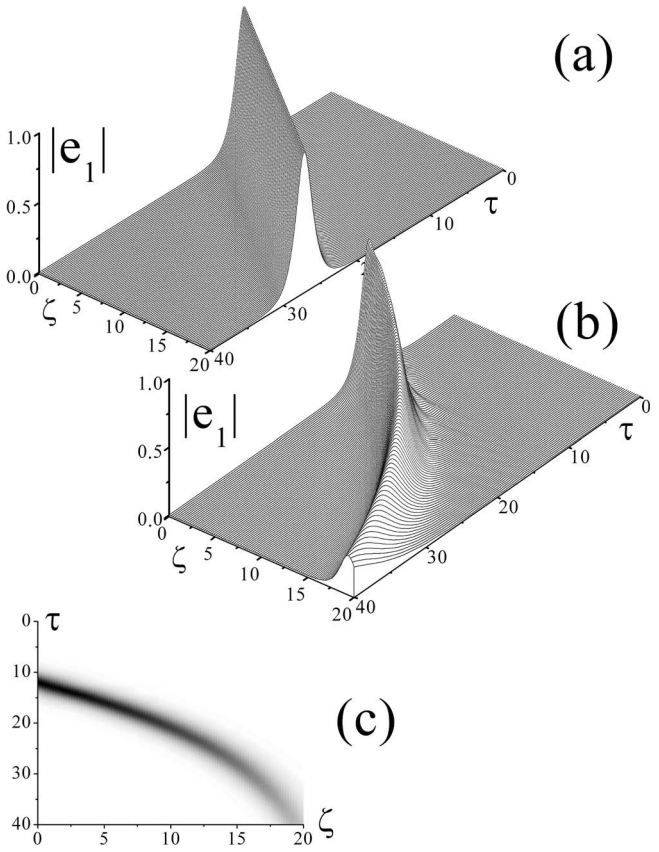

FIG. 1. Self-induced transparency of a circularly polarized wave in an inhomogeneously broadened medium. (a) The local field effect is off, (b) the local field effect is on, and (c) the gray scale map of the process. $\eta=0.5$, $e_{m1}=\infty$, $e_{m2}=0.0$, $\delta=1.0$, $f=1.0$, $\ell_r=1.0$, $\ell_d=\infty$, $\ell_c=\infty$, $\ell_k=\infty$, $\ell_g=\infty$.

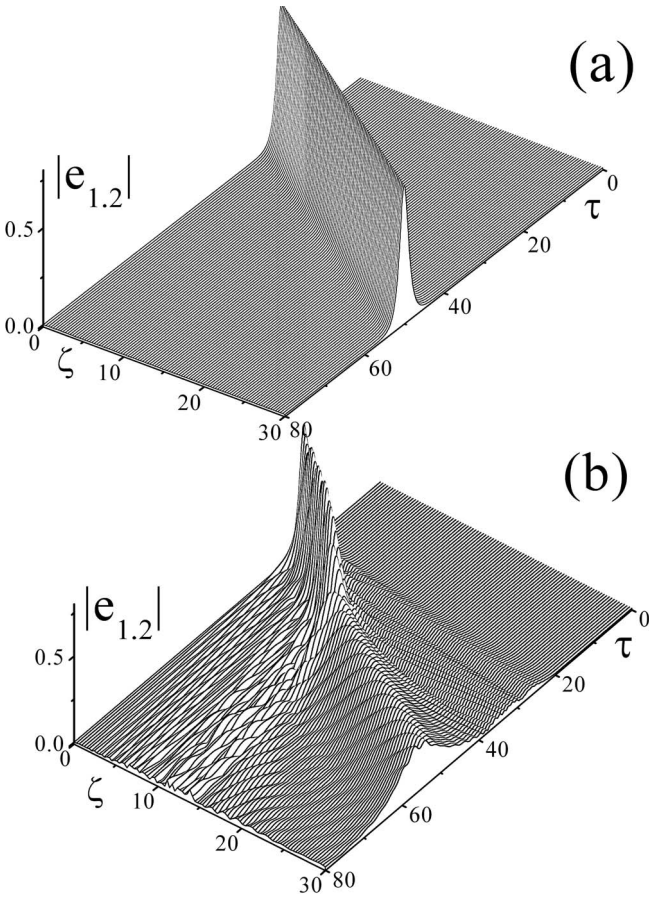

FIG. 2. Self-induced transparency of a linear polarized wave in a homogeneously broadened medium. (a) The local field effect is off; (b) the local field effect is on. $\eta=0.75$, $e_{m1,2}=2^{-1/2}$, $\nu=0$. Other parameters are similar to those in Fig. 1.

resonance coherent interaction, while fiber host material effects are introduced not all at once, but in most cases singly, in order to reveal the individual effect. This approach is justified with the increased opportunity to manage the waveguide parameters in the intensively studied porous photonic band gap optical fibers, especially those filled with resonance gas [29–33].

IV. COHERENT PULSE PROPAGATION IN DOPED FIBER

It is instructive to start with a simple example when there are no fiber effects involved, and the pulse area of the input sech pulse is equal to 2π. The quantum coherency on a certain transition then brings about a net self-induced transparency [Fig. 1(a)] effect. The local field correction introduced in Eq. (3) provides a dynamical shift to the optical resonance of impurities. Under such conditions, a solitary pulse of self-induced transparency ends up as a soliton. The respective nonlinear phase modulation against the inhomogeneous line background leads to the dispersive broadening of the pulse shape [Fig. 1(b)]. The pulse basically keeps the coherency in its interaction with the system of resonance impurities. The optical signal draws a curvilinear trajectory in the (τ,ζ) plane [Fig. 1(c)], experiencing a noticeable slowing down due to the progressing amplitude decrease. The curious feature of the process is the incoherent response in the form of weak residual quasiharmonic radiation detached from the main pulse body.

The simulation in Fig. 2 exhibits the boundary conditions, when the pulse, launched to the homogeneously broadened resonance medium, is linear polarized. In Fig. 2(a) the pulse propagates as a steady-state solitary wave. Each of the circular polarization modes interacts with its individual transition of a degenerated two-level system. Meanwhile, as is seen from Fig. 2(b), the Lorentz field exerts a strong influence on the pulse behavior as it brings a dynamical frequency shift driving a homogeneous ensemble of two-level atoms off the resonance with the propagating field. Thus, there is a deficit of pulse steadiness already in a shallow depth in resonance medium, where a small-scale modulation structure in the pulse-after-action area delivers a reciprocal reaction of resonance atoms. An abrupt fall of the pulse amplitude is evidently due to the lack of energy, which is transferred off the pulse by the resonance interaction process. This automatically reduces the influence of the local field effect and partially restores the coherency. The progressively spreading pulse shape carries the temporal modulation, which could originate from the beat between quantum coherencies on the adjacent transitions.

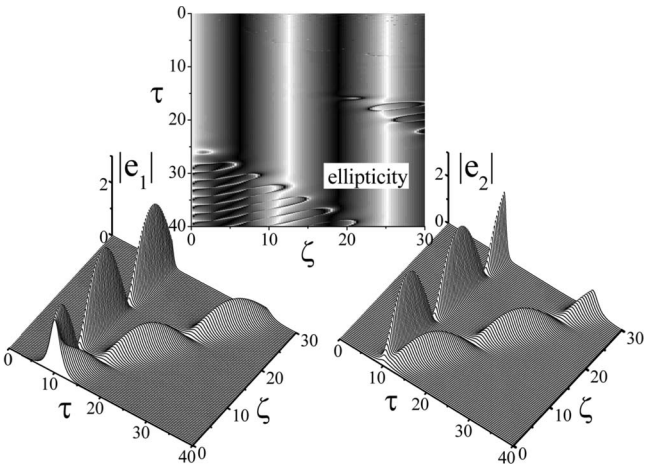

FIG. 3. The influence of the linear birefringence effect on the coherent processes of 4π-pulse breakup in an inhomogeneously broadened resonance medium. $f=1.0$, $\eta=0.0$, $\ell_r=1.0$, $\ell_d=\infty$, $\ell_c=4.0$, $\ell_k=\infty$, $\ell_g=\infty$.

The propagation of the light pulse in birefringent fiber is accompanied by the two-way coupling between the orthogonal counter-rotating polarization modes with the spatial beat period $2\pi(\Delta\beta)^{-1}$ (Fig. 3). This process is featured by the characteristic length ℓ_c in the field equations (1). The cross terms in the model equations (1) responsible for birefringence makes it possible to initiate a circularly polarized wave in one polarization channel by inputting the pulse with opposite polarization. It is remarkable that the coherent interaction of the propagating field with the resonance impurities hardly affects the process of the birefringent beat. The coherent process of 4π-pulse breakup is accompanied by the periodical intermode coupling with the spatial period of energy transfer $\ell_b=\pi\ell_c$ equal to about 12 units (Fig. 3).

The local field is revealed largely in the slowing down and damping of the component with the smaller amplitude [Figs. 4(a)–4(d)], which is similar to Fig. 1(b). The gray scale map of ellipticity ε [Fig. 3 (upper panel)] shows that this function is uniform over the pulse temporal spread and oscillates in the course of its propagation in fiber [21]. The polarization state alters from a linear polarization ($\varepsilon=0$) to a circular polarization of the opposite direction [from $\varepsilon=+1$ (white) to $\varepsilon=-1$ (black)]. The azimuth angle φ (not shown) changes from $-\pi/4$ to $\pi/4$. The ripples by both sides of the pulse propagation area in Fig. 3 (upper panel) are the result of the numerical fluctuations provoking the random switchovers of ellipticity ε on the wings of pulses, where the field of both types of polarizations is extremely weak.

By disregarding the frequency dependence of the index difference between the x and y polarized modes, one obtains $l_c/l_g \approx \lambda/2\pi(ct_p)$. Therefore, it is possible to neglect the pulse walk-off effect for the pulse width in a picosecond range as this phenomenon occurs over a distance, which is much longer than the linear beat length of fiber. However, the polarization mode dispersion can be important in the femtosecond pulse duration domain. For example, for a signal pulse at the carrier wavelength $\lambda=1500$ nm and time duration $t_p=10$ fs, the ratio $l_c/l_g \approx 0.08$, and the characteristic distance of the group velocities mismatch becomes comparable with the length of resonance interaction L_r.

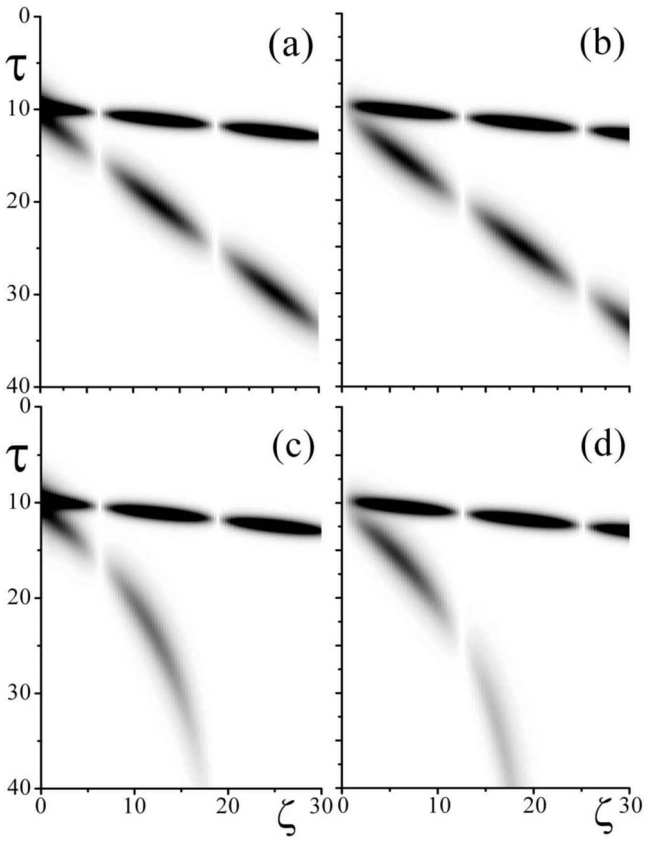

FIG. 4. [(a) and (b)] Gray scale map of the processes, depicted in Fig. 3. [(c) and (d)] The effect of local field ($\eta=0.5$) onto that of 4π-pulse decomposition in an inhomogeneously broadened resonance medium.

The effect of spatial divergence of the differently polarized components initiated by a solitary circularly polarized pulse is demonstrated in Fig. 5. The wave radiation process [Figs. 5(a)–5(c)] in the time moments following the pulse results from the resonance interaction with the impurity atoms [34,46]. The retardation is scaled by the "cooperative" time $t_{cp}=\hbar(4\pi n_a d_{\text{eff}}^2)^{-1}$. In the range of parameters adopted in the model, the inequality $t_{cp} > t_0$ holds. The walk-off effect manifests only as a residual trace clearly because of the expenditure of pulse energy for the interaction with the ensemble of resonance dopants. The polarization properties of the light pulse are displayed in the gray scale map in Fig. 5(b). The out-of-phase counterpolarized radiation occurs in the later time moments due to the resonance coherent interaction with the adjacent transition [Figs. 5(a) and 5(c)]. That gives rise to a strong modulation of ellipticity [Fig. 5(b)] of the polarized wave field [47].

The local field effect [Figs. 5(d)–5(f)] causes the frequency shifts and the degradation of coherency in the interaction of the field with the resonance medium, accompanied by the phase modulation of the polarization components of the spreading field and the small-scale fluctuations of ellipticity [Fig. 5(e)].

For the pulses of the 100 fs range and typical material constants, the length of coherent interaction $L_r^{(2\pi)}$ is compa-

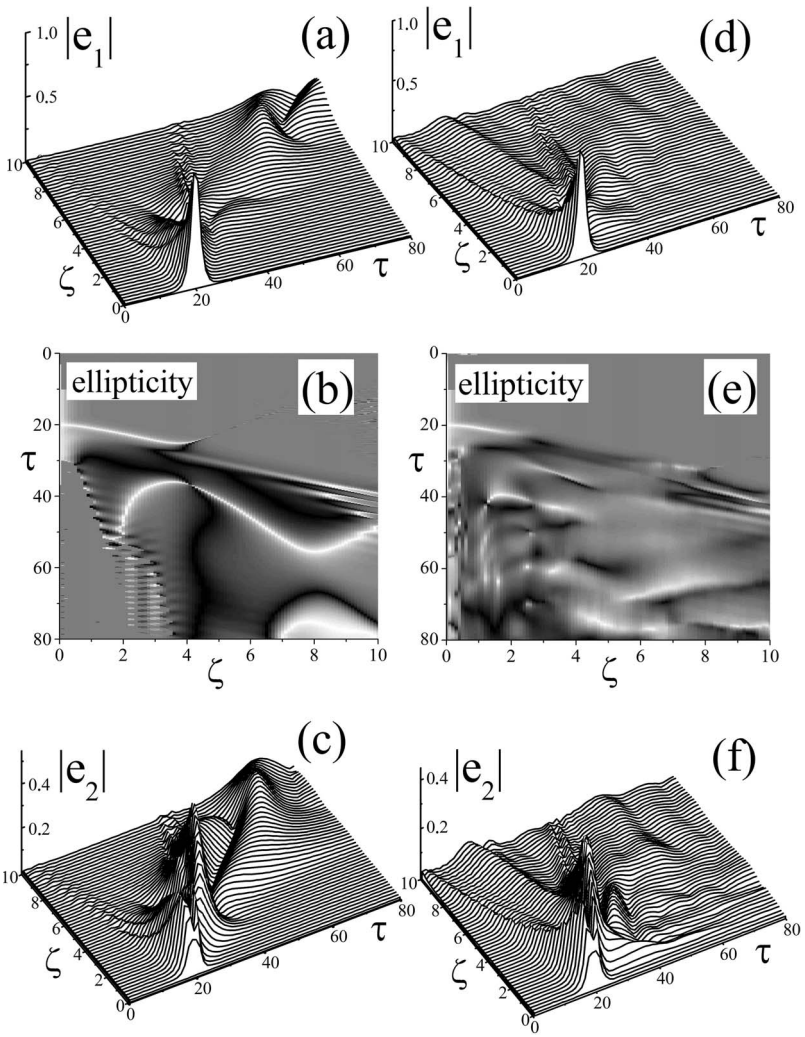

FIG. 5. [(a–c)] The walk-off effect for a circularly polarized input 2π-pulse in an inhomogeneously broadened resonance medium in the absence of Lorentz-field corrections ($\eta=0$). [(d–f)] The same as in (a)–(c) in the presence of the local field effect ($\eta=1.0$). $\ell_r=1.0$, $\ell_d=\infty$, $\ell_c=\infty$, $\ell_k=\infty$, $\ell_g=1.0$, $f=1.0$.

rable with the dispersion length L_d and so the dispersion process cannot be ignored. The dispersion of group velocities of different spectral components of USP distorts the coherent effect of 4π-pulse decomposition [Fig. 6(a)]. This proves in the temporal broadening and generation of quasiharmonic radiation from the area of pulse propagation, though the traces of the coherent process of 4π-pulse decay remain [Fig. 6(b)]. The ripples on the contour of the spreading pulses are partially the artifact, as there is a reflection of quasiharmonic waves on the rigid boundaries back to the computational grid. The availability of local field effect changes dramatically the spatiotemporal dynamics of propagating signals. The absorption line shift, which is proportional to the population difference, drives the two-level atoms out the resonance, thus making the interaction of the field and resonance impurities inefficient with the corresponding loss of coherency. The result is shown in Fig. 6(c), where the well-pronounced picture of the effect of dispersion substitutes the coherent linear polarized 4π-pulse decomposition is displayed in Fig. 6(a).

Figure 7 exhibits a numerical modeling of the situation that is somewhat extreme, when the group velocity dispersion due to the frequency-dependent refractive index of the fiber is weaker than a Kerr nonlinear self-phase modulation. That takes place in short ordinary fibers not sufficient for dispersion to develop, or the enhancement of nonlinearity can be achieved in photonic band-gap fibers filled with active gas [30]. In order to enforce the effect, the normalized length of the Kerr nonlinearity is chosen shorter than the reference length of resonance absorption $\ell_k=0.1\ell_r$. The intensity-dependent nonlinear phase modulation brings the typical changes in temporal shape of the pulse: the small-scale spike structure on the trailing edge of the pulse and the predictable steep slope of the leading edge. Nevertheless the collapse of the pulse shape, which would have been forecasted in this situation, does not occur. The trailing edge is obviously wider as the result of a different type of dispersion owed to resonance interaction with the inhomogeneous ensemble of two-level atoms. The demonstrative coherent interaction process of 4π-pulse decomposition [Fig. 7(a)], having started at the input of fiber, does not develop further due to a strong phase modulation [Fig. 7(b)]. As there is no radiation in the temporal domain after the pulse action, one could assume that the resonance atoms are restored in the initial state and the coherence of the light-medium interaction is not violated. The incorporation of local field effect into the model leads to the noticeable alterations in pulse dynamics [Fig. 7(c)]. The defect of resonance, ensued from the frequency shifts of the individual two-level system summarized over the inhomogeneous line, releases the dispersion in resonance subsystem,

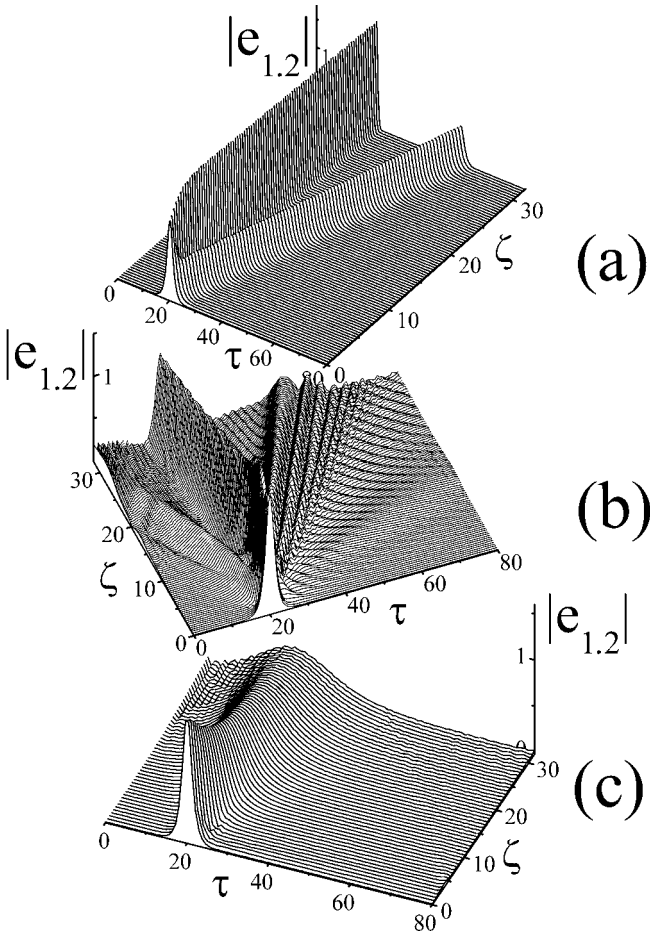

FIG. 6. (a) Linear polarized 4π-pulse breakup net effect on a homogeneous line ($\nu=0$); (b) the same effect in the presence of dispersion ($\eta=0$); (c) the effect of local field correction on the process that is shown in panel (b). $\eta=5.0$, $e_{m1,2}=2^{1/2}$, $\ell_r=1.0$, $\ell_d=5.0$, $\ell_c=\infty$, $\ell_k=\infty$, $\ell_g=\infty$, $f=1.0$.

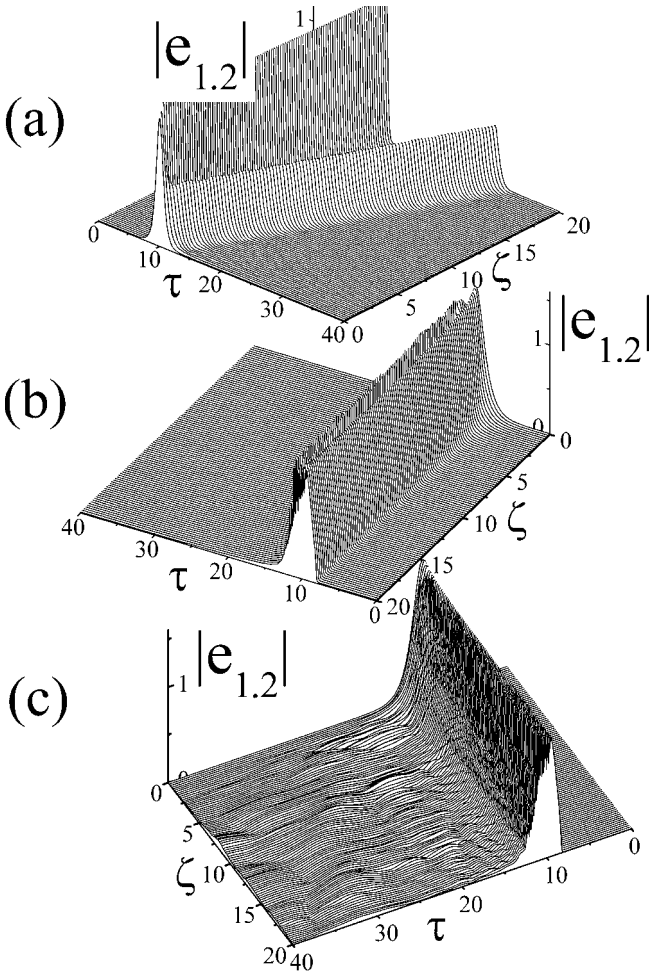

FIG. 7. (a) Linear polarized 4π-pulse breakup net effect on an inhomogeneous line; (b) the same input pulse coupled to the Kerr medium; (c) the effect of local field correction on the process that is shown in panel (b). $\eta=1.0$, $e_{m1,2}=2^{1/2}$, $\ell_r=1.0$, $\ell_d=\infty$, $\ell_c=\infty$, $\ell_k=1.0$, $\ell_g=\infty$, $f=1.0$.

which manifests in a weak quasiharmonic radiation at the pulse after-action moments of time.

V. PHOTON-ECHO EFFECT IN RESONANT FIBER

Echo studies are particularly advantageous in fiber geometry since long interaction lengths are available, phase matching is intrinsically satisfied, and the small core size results in modest power requirements. Photon-echo [48] is generated in an inhomogeneous ensemble of resonance particles. The pulse of coherent spontaneous radiation is the result of the dephasing under the action of the first USP and the subsequent rephasing of radiators under the action of a second pulse at the time moment approximately double to the time interval between pulses.

While propagating down a fiber the echo pulse is developing into a full-scaled signal with the energy sufficient for the excitation of subsequent multiple echoes. This effect is clearly introduced in Fig. 8, where the equidistant series of echo pulses follows the $\pi/2$ and π excitation pulses. As soon as the modulus of field amplitude is plotted in Fig. 8, some extra humps between the echo pulses show traces of the negative nutational surges of field amplitude. The remarkable and new feature of Fig. 8 is that at the distance of several absorption lengths, where the excitation pulses exhaust, the energy, coupled to the fiber at the entrance, completely repumps in coherent spontaneous radiation of the primary photon-echo signal and multiple echoes. In the depth of the medium, the echoes merge to develop into a steady-state pulse with low amplitude and a high speed of retardation. The introduction of birefringence in multiple echo gives rise to a different effect, when the photon echo appears in the conjugated polarization channel (Fig. 9), which has not been initially activated by a pair of USPs. The signals of multiple echo participate in the process of back and forth coupling between two polarization states with the appropriate beat period.

Under the Kerr effect (Fig. 10) the duration of the excitation pulses shortens and the temporal shape of the weak first pulse suffers distortion and damping. The excitation pulses do not shift along the computational time grid; Kerr nonlinearity suppresses the weak nutations characteristic for coher-

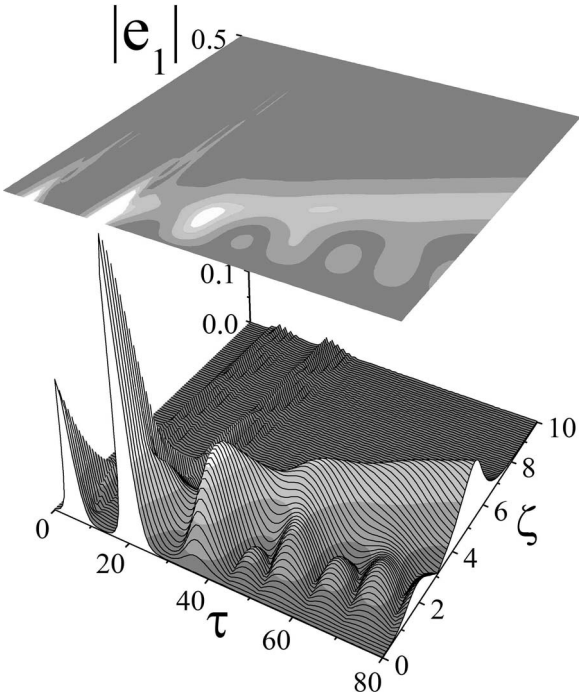

FIG. 8. Pure multiple photon-echo effect in one polarization mode in an optically extended medium. $f=1.0$, $\eta=0.0$, $\ell_r=1.0$, $\ell_d=\infty$, $\ell_c=\infty$, $\ell_k=\infty$, $\ell_g=\infty$.

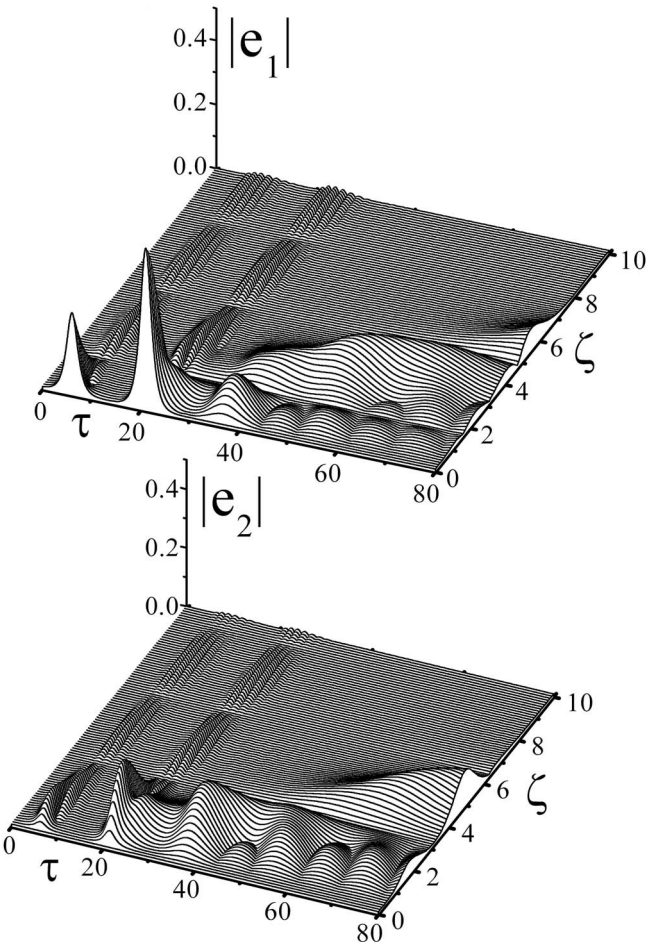

FIG. 9. Multiple photon-echo effect in an optically extended medium in the presence of linear birefringence. $f=1.0$, $\eta=0.0$, $\ell_r=1.0$, $\ell_d=\infty$, $\ell_c=4.0$, $\ell_k=\infty$, $\ell_g=\infty$.

ent interaction with resonance medium (see Figs. 8 and 9). The first pulse is getting too weak to noticeably excite the spectral components of the resonance line; so the perceptible multiple photon-echo effect is observed only in the short distance of propagation in resonant fiber and then it vanishes.

Photon-echo effect keeps its identity in the presence of the full set of main fiber effects: birefringence, Kerr-nonlinearity, material dispersion, and walk-off effect. Figure 11 clearly shows the rise of primary photon-echo in fiber, in which the birefringence initiates the photon-echo effect in the conjugated polarization state. The cubic nonlinearity causes a squeezing of temporal shape of the propagating pulses accompanied with the well-recognized oscillations on the wings of the excitation pulse due to dispersion.

VI. CONCLUSION

In conclusion, the propagation of USPs of elliptically polarized light in nonlinear doped birefringent fiber has been numerically examined. The resonance impurities in the form of two-level atoms are included in the model in addition to the full set of fiber effects. The local field effect is phenomenologically taken into account. The coherent resonance interaction of USPs with an inhomogeneously broadened subsystem of resonance impurities is considered as the basic phenomenon influenced by the conventional fiber factors: host material dispersion, cubic nonlinearity, birefringence, and walk-off effect. The numerical modeling has been performed for two types of coherent transients: self-induced transparency, specifically the 4π-sech pulse breakup, and the photon-echo effect. By choosing the type of polarization of the launched pulses, one can excite either a separate transition in the degenerated two-level quantum system or both adjacent transitions. The presence of linear birefringence and spatial divergence of differently polarized components of optical pulse (walk-off effect) leads to the coupling of coherent radiation to the conjugated polarization mode. Remarkably, the linear birefringence would not affect a steadiness of the 4π-decay process if there is no Lorentz-field correction.

The local field effect provokes the dynamical frequency shift on the background of a wide resonance absorption line, which broadly leads to the partial loss of coherency especially well seen in small-scale spatiotemporal variations of ellipticity in the field of a propagating wave. The group-velocity dispersion effect is not able to destroy a coherent transient but it imposes the inherent temporal broadening and the oscillations on the shape of the USP. The nonlinear Kerr effect suppresses the coherent process of pulse breakup as a result of significant squeezing of pulse shape and the shortening of its duration.

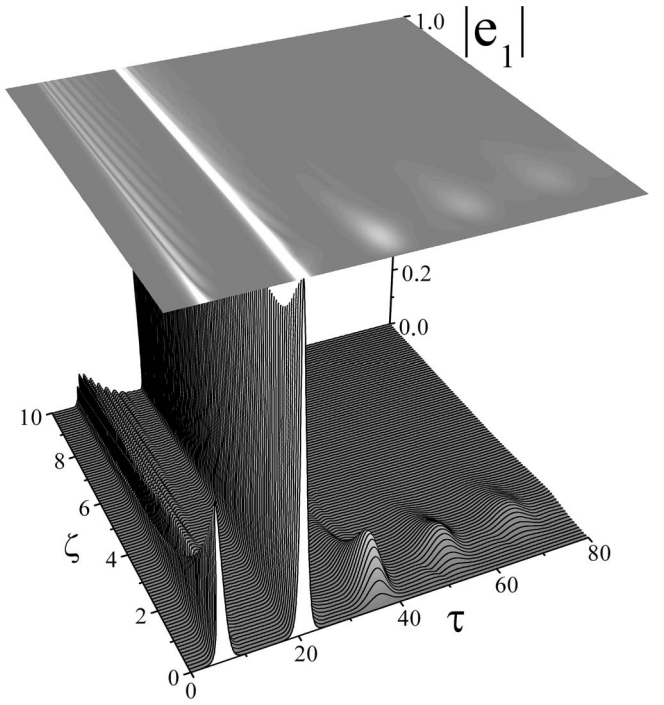

FIG. 10. Multiple photon-echo effect in an optically extended medium in the presence of Kerr effect. $f=1.0$, $\eta=0.0$, $\ell_r=1.0$, $\ell_d=\infty$, $\ell_c=\infty$, $\ell_k=1.0$, $\ell_g=\infty$.

The most interesting result in photon-echo numerics is the emergence of a steady-state signal out from the series of multiple photon echoes forming in an optically extended medium of active fiber. Attention should be also drawn to the fact that due to the intrinsic fiber birefringence there is a possibility to excite photon echo of the conjugated polarization mode, even if this mode is not activated by the input pulses. The temporal and polarization features of the conventional coherent transients, considered in this work, may become important in light of renewed interest in fiber optics due to the development of photon-crystal fiber and metamaterial physics.

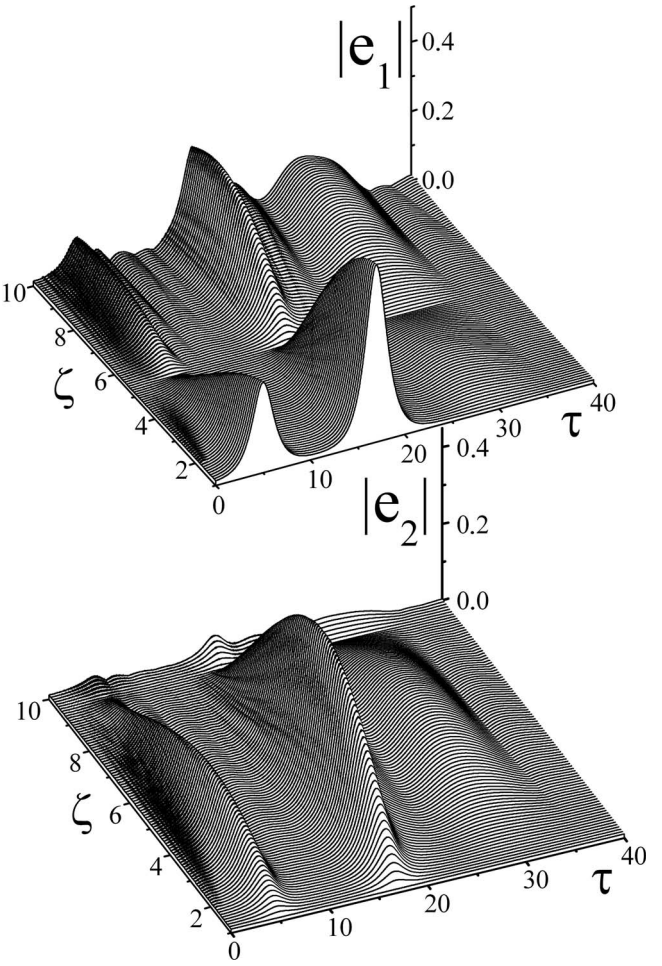

FIG. 11. Photon-echo in a nonlinear birefringent resonance impurity-doped fiber. $f=1.0$, $\eta=0.0$, $\ell_r=1.0$, $\ell_d=10.0$, $\ell_c=0.3$, $\ell_k=1.25$, $\ell_g=75.0$.

ACKNOWLEDGMENTS

The author gratefully acknowledges the fruitful discussions with Andrei I. Maimistov and Askhat M. Basharov. The research is supported by the Russian Foundation for Basic Research (Grant No. 06-02-16406).

[1] S. L. McCall and E. L. Hahn, Phys. Rev. **183**, 457 (1969).
[2] A. M. Basharov and A. I. Maimistov, Opt. Spectrosc. **66**, 167 (1989).
[3] A. I. Maimistov, A. M. Basharov, S. O. Elyutin, and Yu. M. Sklyarov, Phys. Rep. **191**, 1 (1990).
[4] M. Nakazawa, Y. Kimura, K. Kurokawa, and K. Suzuki, Phys. Rev. A **45**, R23 (1992).
[5] M. Nakazawa, K. Suzuki, Y. Kimura, and H. Kubota, Phys. Rev. A **45**, R2682 (1992).
[6] M. Nakazawa, K. Suzuki, H. Kubota, and Y. Kimura, Opt. Lett. **18**, 613 (1993).
[7] I. V. Mel'nikov, R. F. Nobiev, and A. V. Nazarkin, Opt. Lett. **15**, 1348 (1990).
[8] A. I. Maimistov, Sov. J. Quantum Electron. **22**, 271 (1992).
[9] A. I. Maimistov, Opt. Spectrosc. **72**, 631 (1992).
[10] V. V. Kozlov and E. E. Fradkin, Opt. Lett. **20**, 2165 (1995).
[11] E. V. Kazantseva, A. I. Maimistov, S. O. Elyutin, and S. Wabnitz, J. Opt. Soc. Am. B **24**, 559 (2007).
[12] A. I. Maimistov and A. M. Basharov, Izv. Ross. Akad. Nauk, Ser. Fiz. **62**, 354 (1998).
[13] A. M. Basharov and A. I. Maimistov, Opt. Spectrosc. **88**, 380 (2000).
[14] K. Porsezian and K. Nakkeeran, Phys. Rev. Lett. **74**, 2941 (1995).
[15] D. V. Skryabin, A. V. Yulin, and A. I. Maimistov, Phys. Rev. Lett. **96**, 163904 (2006).

[16] V. N. Serkin, A. Hasegawa, and T. L. Belyaeva, Phys. Rev. Lett. **98**, 074102 (2007).
[17] J. Hegarty, M. M. Broer, B. Golding, J. R. Simpson, and J. B. MacChesney, Phys. Rev. Lett. **51**, 2033 (1983).
[18] V. L. da Silva, Y. Silberberg, J. P. Heritage, E. W. Chase, M. A. Saifi, and M. J. Andrejco, Opt. Lett. **16**, 1340 (1991).
[19] V. L. daSilva and Y. Silberberg, Phys. Rev. Lett. **70**, 1097 (1993).
[20] A. D. Boardman and G. S. Cooper, J. Opt. Soc. Am. B **5**, 403 (1988).
[21] H. G. Winful, Appl. Phys. Lett. **47**, 213 (1985).
[22] S. Trillo, S. Wabnitz, E. M. Wright, and G. I. Stegeman, Opt. Commun. **70**, 166 (1989).
[23] S. O. Elyutin and A. I. Maimistov, Chaos, Solitons Fractals **11**, 1253 (2000).
[24] C. Pare and M. Florjan'czyk, Phys. Rev. A **41**, 6287 (1990).
[25] B. A. Malomed, Phys. Rev. A **43**, 410 (1991).
[26] D. J. Muraki and W. L. Kath, Physica D **48**, 53 (1991).
[27] A. I. Maimistov and S. O. Elyutin, J. Mod. Opt. **39**, 2193 (1992).
[28] D. J. Kaup, B. A. Malomed, and R. S. Tasgal, Phys. Rev. E **48**, 3049 (1993).
[29] A. M. Zheltikov, Phys. Usp. **45**, 687 (2002).
[30] D. V. Skryabin, F. Biancalana, D. M. Bird, and F. Benabid, Phys. Rev. Lett. **93**, 143907 (2004).
[31] S. Ghosh, J. E. Sharping, D. G. Ouzounov, and A. L. Gaeta, Phys. Rev. Lett. **94**, 093902 (2005).
[32] P. Benabid, S. Light, F. Couny, and P. St. J. Russell, Opt. Express **13**, 5694 (2005).
[33] D. G. Ouzounov, F. R. Ahmad, D. Muller, N. Venkataraman, M. T. Gallagher, M. G. Thomas, J. Silcox, K. W. Koch, and A. L. Gaeta, Science **301**, 1702 (2003).
[34] M. D. Crisp, Phys. Rev. A **1**, 1604 (1970).
[35] Y. Ben-Aryeh, C. M. Bowden, and J. C. Englund, Phys. Rev. A **34**, 3917 (1986).
[36] C. M. Bowden and J. P. Dowling, Phys. Rev. A **47**, 1247 (1993).
[37] A. A. Afanas'ev, R. A. Vlasov, O. K. Khasanov, T. V. Smirnova, and O. M. Fedotova, J. Opt. Soc. Am. B **19**, 911 (2002).
[38] A. I. Maimistov and E. A. Manykin, Sov. Phys. JETP **58**, 685 (1983).
[39] M. Nakazawa, E. Yamada, and H. Kubota, Phys. Rev. A **44**, 5973 (1991).
[40] D. P. Caetano, S. B. Cavalcanti, and J. M. Hickmann, Phys. Rev. E **65**, 036617 (2002).
[41] S. Chi, T.-Y. Wang, and S. Wen, Phys. Rev. A **47**, 3371 (1993).
[42] E. J. S. Fonseca, S. B. Cavalcanti, and J. M. Hickmann, Phys. Rev. E **64**, 016610 (2001).
[43] S. O. Elyutin and A. I. Maimistov, J. Exp. Theor. Phys. **93**, 737 (2001).
[44] C. R. Menyuk, IEEE J. Quantum Electron. **25**, 2674 (1989).
[45] C. R. Menyuk, IEEE J. Quantum Electron. **23**, 174 (1987).
[46] L. Allen and J. H. Eberly, *Optical Resonance and Two-Level Atoms* (Wiley, New York, 1975).
[47] H. Steudel, J. Mod. Opt. **35**, 693 (1988).
[48] D. Abella, N. A. Kurnit, and S. R. Hartmann, Phys. Rev. **141**, 391 (1966).